

Triply deuterated ammonia in NGC 1333

F.F.S. van der Tak¹, P. Schilke¹, H.S.P. Müller², D.C. Lis³, T.G. Phillips³, M. Gerin^{4,5}, and E. Roueff⁵

¹ Max-Planck-Institut für Radioastronomie, Auf dem Hügel 69, 53121 Bonn, Germany

² I. Physikalisches Institut, Universität zu Köln, 50937 Köln, Germany

³ California Institute of Technology, Downs Laboratory of Physics 320-47, Pasadena, CA 91125, USA

⁴ Lab. de Radioastronomie Millimétrique, Dépt. de Physique de l'E.N.S., 24 Rue Lhomond, 75231 Paris, France

⁵ DEMIRM, Observatoire de Paris, 61 avenue de l'Observatoire, 75014 Paris, France

Received April 1, 2002; accepted April 24, 2002

Abstract. The Caltech Submillimeter Observatory has detected triply deuterated ammonia, ND₃, through its $J_K = 1_0^a \rightarrow 0_0^s$ transition near 310 GHz. Emission is found in the NGC 1333 region, both towards IRAS 4A and a position to the South-East where DCO⁺ peaks. In both cases, the hyperfine ratio indicates that the emission is optically thin. Column densities of ND₃ are $3 - 6 \times 10^{11} \text{ cm}^{-2}$ for $T_{\text{ex}}=10$ K and twice as high for $T_{\text{ex}}=5$ K. Using a Monte Carlo radiative transfer code and a model of the structure of the IRAS source with temperature and density gradients, the estimated ND₃ abundance is 3.2×10^{-12} if ND₃/H₂ is constant throughout the envelope. In the more likely case that ND₃/H₂D⁺ is constant, ND₃/H₂ peaks in the cold outer parts of the source at a value of 1.0×10^{-11} . To reproduce the observed NH₃/ND₃ abundance ratio of ~ 1000 , grain surface chemistry requires an atomic D/H ratio of ≈ 0.15 in the gas phase, >10 times higher than in recent chemical models. More likely, the deuteration of NH₃ occurs by ion-molecule reactions in the gas phase, in which case the data indicate that deuteron transfer reactions are much faster than proton transfers.

Key words. ISM: abundances – ISM: molecules

1. Introduction

Deuterium-bearing molecules have attracted attention in recent years. Physically, they appear to be good probes of the very cold phases of molecular clouds prior to star formation. Chemically, the isotopic composition of molecules is an important clue to their formation mechanism. There are two ways to make deuterated molecules. First, at temperatures $\lesssim 70$ K, the gas-phase reaction equilibrium $\text{H}_3^+ + \text{HD} \rightleftharpoons \text{H}_2\text{D}^+ + \text{H}_2$ is shifted in the forward direction. Subsequent deuteron transfer from H₂D⁺ to, e.g., CO and N₂, leads to the large observed abundance ratios of DCO⁺/HCO⁺ and N₂D⁺/N₂H⁺ of ~ 0.1 , four orders of magnitude higher than the Galactic D/H ratio (Turner 2001). The key species of this chemical scheme, H₂D⁺, was recently detected in the Class 0 source NGC 1333 IRAS 4A (Stark et al. 1999). The high densities and low temperatures in this object promote the formation of H₂D⁺ out of H₃⁺ and HD, and also prevent its destruction because the major destroyer of H₂D⁺, CO, is depleted by a factor of ~ 100 due to freeze-out onto dust grains.

Alternatively, deuterium-bearing molecules can be formed on dust grains by surface chemistry. Accretion of

H and CO onto grains, followed by reaction, is thought to produce solid H₂CO and CH₃OH. This mechanism favours deuteration because the atomic D/H ratio in the gas phase is much greater than the elemental ratio. The observed abundances of HDCO, CH₃OD and D₂CO in Orion and IRAS 16293 indicate their synthesis on dust grains (Turner 1990; Charnley et al. 1997; Ceccarelli et al. 1998). The same mechanism may work for NH₃, provided most nitrogen is in atomic form, and support for this route comes from detections of solid NH₃ (Lacy et al. 1998; Gibb et al. 2000). However, these detections remain tentative (Dartois & d'Hendecourt 2001), and observations of N₂H⁺ suggest that in dense clouds, most nitrogen is in molecular form (Womack et al. 1992).

While NH₂D has been observed in many sources (Saito et al. 2000; Shah & Wootten 2001), ND₂H has only been detected so far towards the cold, starless cores L134N and L1689N (Roueff et al. 2000; Loinard et al. 2001). The temperatures in these sources of ≈ 10 K are too low for significant evaporation of even the most volatile ices to occur. Gas-phase reactions can probably account for the observed abundance ratios (Rodgers & Charnley 2001), but observations of ND₃ would present a strong test, as the gas-phase route produces ≈ 3 times more ND₃ than the grain surface route. As a step towards measuring the relative importance of gas-phase and solid-state deuteration, we have observed the $J_K = 1_0 \rightarrow 0_0$ transition of

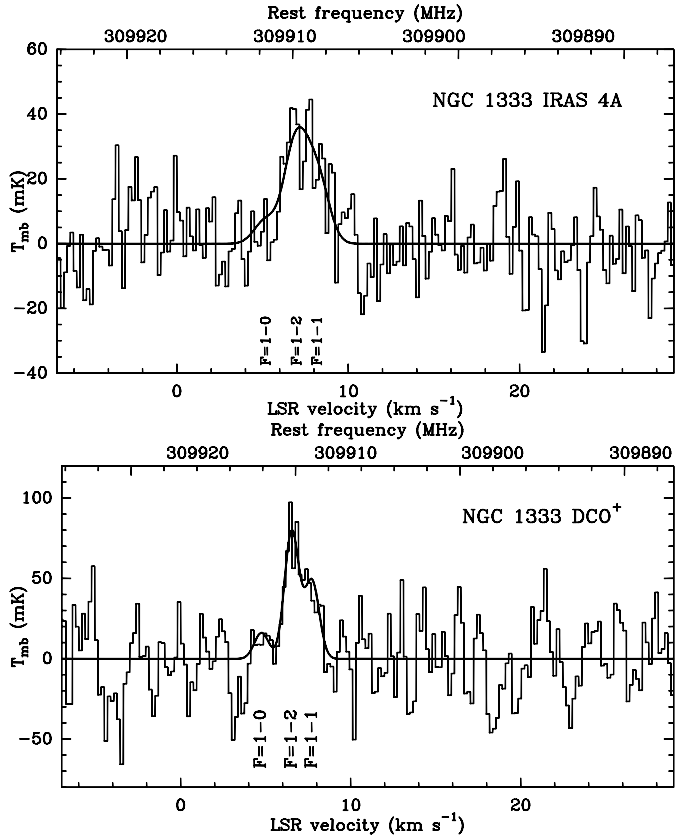


Fig. 1. Top: Spectrum of NGC 1333 IRAS 4A near 309.9 GHz, taken with the CSO, with the 3-component fit described in the text overlapped and the expected positions of the hyperfine components of the ND_3 $J_K = 1_0^a \rightarrow 0_0^s$ line indicated. Bottom: Spectrum taken at the $(+23, -06)''$ offset position, where DCO^+ peaks.

ND_3 towards NGC 1333. Together with similar observations towards Barnard 1 by Lis et al. (2002), this is the first detection of a triply deuterated molecule in interstellar space.

2. Observations and Results

The rotational energy levels of symmetric top molecules are labeled by the total angular momentum J and its projection on the molecular symmetry axis K . For NH_3 and ND_3 , inversion motion splits each level further into states which are symmetric (s) and antisymmetric (a) upon reflection in the plane of the H or D atoms. The measured frequencies of the ND_3 $J_K = 1_0^a \rightarrow 0_0^s$ transition are 309908.46 ($F=1 \rightarrow 1$), 309909.69 ($F=2 \rightarrow 1$) and 309911.53 ($F=0 \rightarrow 1$) MHz; those of the $J_K = 1_0^s \rightarrow 0_0^a$ transition are 306735.58 ($F=1 \rightarrow 1$), 306736.96 ($F=2 \rightarrow 1$) and 306738.95 ($F=0 \rightarrow 1$) MHz (Helminger & Gordy 1969). Due to spin statistics, the $J_K = 1_0^a \rightarrow 0_0^s$ transition is stronger than the $J_K = 1_0^s \rightarrow 0_0^a$ transition by a factor of 10.

The Caltech Submillimeter Observatory (CSO) is a 10.4-m single-dish antenna located atop Mauna Kea, Hawaii. At 310 GHz, the CSO has an FWHM beam size

of $25''$, slightly larger than the diffraction limit. Initial observations of ND_3 $J_K = 1_0^a \rightarrow 0_0^s$ toward NGC 1333 IRAS 4A ($\alpha_{2000} = 03^h 29^m 10^s.3$, $\delta_{2000} = +31^\circ 13' 32''$) were carried out December 5–8, 2001. Additional data were taken January 24, 2002, with the local oscillator frequency shifted to verify the sideband origin of detected features. Weather conditions were average with zenith opacities of ≈ 0.1 at 225 GHz. An IF frequency of 1594 MHz was used to put the $J_K = 1_0^s \rightarrow 0_0^a$ transition in the image sideband. To subtract atmospheric and instrumental background, positions $240''$ offset were observed using the chopping secondary mirror. The main beam efficiency at the time of observations, measured through observations of Saturn, was 64%, using a planetary brightness temperature of 135 K at 310 GHz.

Figure 1 (top) shows the combined data from all nights, aligned in signal frequency. This spectrum represents 151 minutes of on-source integration with a mean T_{sys} of 521 K and a source elevation of 44° . A feature is detected at 309909.4 MHz, at which frequency neither the JPL (Pickett et al. 1998, spec.jpl.nasa.gov) nor the CDMS (Müller et al. 2001, www.cdms.de) catalog lists any plausible molecular lines other than ND_3 . The 307 GHz component is not detected to $T_{\text{mb}} < 14$ mK (1σ).

Data were also obtained at a position $23''$ East and $6''$ South of the IRAS 4A position, which is where the DCO^+ $3 \rightarrow 2$ emission peaks (Lis et al., in preparation). The bottom panel of Figure 1 shows that the ND_3 line is also somewhat stronger than at the IRAS 4A position. The noise level for this spectrum is 23 mK (1σ).

Lines of ND_3 exhibit hyperfine structure due to coupling of the ^{14}N nuclear spin with the rotational angular momentum. Splitting due to D, owing to its small quadrupole moment, is only ≈ 200 kHz and remains unresolved in our data. Thus, we have fitted the observed spectrum with three Gaussian profiles with optical depth ratios of 5:3:1 and assuming that the components have equal widths and excitation temperatures. Such a fit has four parameters: optical depth τ , central velocity V_0 , line width ΔV and intensity $T_{\text{mb}} = \tau(T_{\text{ex}} - T_{\text{bg}})$. We used the HFS method inside the CLASS package. Leaving all parameters free gives the values reported in columns 2–5 of Table 1. For the IRAS 4A position, fixing V_0 and/or ΔV to values measured in other lines, 7.0 and 1.2 km s^{-1} (Blake et al. 1995) gives similar results. The fit results indicate that the line shape is consistent with the optically thin hyperfine intensity ratio of 5:3:1, but that the signal to noise is not high enough to constrain the optical depth. Without taking hyperfine broadening into account, ΔV at the IRAS 4A position would be 2.6 km s^{-1} , much broader than other lines from the cold component of this source (Blake et al. 1995). The line shape thus confirms the assignment of the line to ND_3 .

From the observed line strengths integrated between 3.5 and 10.0 km s^{-1} , given in column 6 of Table 1, we estimate the ND_3 column density assuming an excitation temperature $T_{\text{ex}} = 10$ K. In the optically thin limit, but outside the Rayleigh-Jeans regime, and using a background tem-

Table 1. Line parameters^a

Position	τ	V_0 km s ⁻¹	ΔV km s ⁻¹	$T_{\text{mb}}\tau$ mK	$\int T_{\text{mb}}dV$ mK km s ⁻¹	$N(T_{\text{ex}}=10 \text{ K})$ 10 ¹¹ cm ⁻²	$N(T_{\text{ex}}=5 \text{ K})$ 10 ¹¹ cm ⁻²
IRAS 4A	0.6(20)	7.0(2)	1.6(6)	81(62)	71(21)	2.9(9)	6.3(19)
DCO ⁺	0.1(27)	6.5(1)	1.0(2)	149(22)	144(43)	5.9(18)	12.8(38)

^a Numbers in brackets denote the uncertainty in units of the last decimal

perature of $T_{\text{bg}} = 2.7 \text{ K}$, the velocity-integrated optical depth follows from

$$\int T_{\text{mb}}dV = \frac{h\nu}{k} \left(\frac{1}{e^{h\nu/kT_{\text{ex}}} - 1} - \frac{1}{e^{h\nu/kT_{\text{bg}}} - 1} \right) \int \tau dV$$

so that

$$\int \tau dV = \frac{c^3}{8\pi\nu^3} AN_u (e^{h\nu/kT_{\text{ex}}} - 1)$$

with

$$N_u = \frac{g_u N}{Q(T_{\text{ex}})} e^{-E_{\text{up}}/kT_{\text{ex}}}$$

yields the column density estimates in column 7 of Table 1. Here, $Q(T_{\text{ex}})$ is the partition function $\sum_i g_i e^{-E_i/kT_{\text{ex}}}$, equal to 38.3 for $T_{\text{ex}}=10 \text{ K}$. The Einstein A coefficient of $2.57 \times 10^{-4} \text{ s}^{-1}$ follows from the dipole moment of 1.49 D (di Lonardo & Trombetti 1981).

The assumed value of T_{ex} represents a kinetic temperature at which chemical fractionation should be efficient. However, at densities well below the critical density of this line, $10^7 - 10^8 \text{ cm}^{-3}$, T_{ex} will drop below T_{kin} , which changes the column density estimate. As an example, the last column of Table 1 gives the values for $T_{\text{ex}}=5 \text{ K}$.

3. Abundance of ND₃

To estimate the abundance of ND₃ we have used the Monte Carlo radiative transfer program by Hogerheijde & van der Tak (2000, talisker.as.arizona.edu/~michiel/ratran.html). Lacking auxiliary data on the DCO⁺ position, we concentrate on NGC 1333 IRAS 4A, for which we take the temperature and density structure from Stark et al. (1999). Between the outer and inner radii of 3100 and 10 AU, temperatures increase from 13 to 320 K, and densities from 2×10^6 to $4 \times 10^{11} \text{ cm}^{-3}$; $N(\text{H}_2)=3.1 \times 10^{23} \text{ cm}^{-2}$ in a 13'' beam, but strongly depends on beam size due to the R^{-2} density distribution. The radiative transfer model for ND₃ includes the 30 terms up to 100 cm⁻¹ above ground, including the inversion splitting but not the hyperfine structure. Rate coefficients for de-excitation of NH₃ in collisions with H₂ from Danby et al. (1988) are used, scaled to the different reduced mass of the ND₃-H₂ system, and augmented with the terms that are Pauli-forbidden in NH₃, and with transitions that would be ortho-para conversions in NH₃. Initially, a constant abundance of ND₃ (relative to H₂) was assumed. The

excitation of ND₃ as a function of radius is calculated with the Monte Carlo program. The result is integrated over the line of sight and convolved with a 25'' beam. The area under the synthetic line profile matches the observed value for ND₃/H₂ = 3.2×10^{-12} .

As an alternative model, the ND₃ abundance was assumed to follow that of H₂D⁺. The major chemical formation path to ND₃ starts with the reaction of NH₃ with H₂D⁺ and its derivatives DCO⁺ and N₂D⁺, and proceeds through NH₂D and ND₂H. As a simple way to model this behaviour, we have assumed a constant H₂D⁺/ND₃ ratio. However, this ratio would vary in the case of a varying NH₃ abundance, and if the alternative route starting with the reaction of N⁺ with HD competes, which is slightly endothermic. In the absence of sufficient constraints, we keep H₂D⁺/ND₃ constant. Our two assumed ND₃ abundance profiles could be tested indirectly by observations of key deuterated molecules such as DCO⁺ and N₂D⁺.

The H₂D⁺ abundance profile in NGC 1333 IRAS 4A was calculated analytically by Stark et al. (1999), using assumed values for the cosmic-ray ionization rate ($\zeta = 5 \times 10^{-17} \text{ s}^{-1}$) and the abundances of HD (2.8×10^{-5}) and D (2.8×10^{-6}), and using a CO abundance of 4×10^{-6} estimated from C¹⁷O data. Due to the small energy difference between H₃⁺ and H₂D⁺, the H₂D⁺ abundance is strongly peaked toward large radii where temperatures are low. We have re-calculated the H₂D⁺ abundance profile using $\zeta = 2.6 \times 10^{-17} \text{ s}^{-1}$, the mean of the values implied by observations of H₃⁺ and H¹³CO⁺ towards seven massive young stars (van der Tak & van Dishoeck 2000). This calculation also includes dust radiation which the one by Stark et al. (1999) did not. The new calculations are still consistent with the measured H₂D⁺ line flux, and indicate an H₂D⁺ abundance increasing from 5×10^{-19} at a radius of 10 AU to 5×10^{-10} at $R = 3100 \text{ AU}$. To model the ND₃ data, models were run for several values of the H₂D⁺:ND₃ ratio, and agreement between observed and calculated line flux was found for H₂D⁺/ND₃=46. The ND₃ abundance at large radii is then 1.0×10^{-11} , a factor of 3 higher than that found assuming a constant ND₃ abundance.

4. Chemistry of ND₃

Table 2 summarizes the measured column densities of NH₃ isotopomers toward NGC 1333 IRAS 4A. It is seen that $N(\text{NH}_3)/N(\text{NH}_2\text{D}) \approx 10$ and $N(\text{NH}_3)/N(\text{ND}_3) \approx 1000$; no observations of ND₂H exist yet. The available data suggest a trend where with each H→D substitution, the column density drops by an order of magnitude. Current models of gas-phase chemistry, on the other hand, predict

Table 2. Column densities of ammonia isotopomers towards NGC 1333 IRAS 4A

Species	N cm^{-2}	Beam "	Reference
NH ₃	$3.1(4) \times 10^{14}$	74	Shah & Wootten (2001)
NH ₂ D	$2.2(7) \times 10^{13}$	90	Shah & Wootten (2001)
ND ₃	$2.9(9) \times 10^{11}$	25	this work

that $\text{ND}_2\text{H}/\text{ND}_3 > \text{NH}_2\text{D}/\text{ND}_2\text{H} > \text{NH}_3/\text{NH}_2\text{D}$ (Rodgers & Charnley 2001), unless deuterium transfer reactions are much more rapid than proton transfers. The same trend is expected in the case of grain surface chemistry. However, the measured column densities are uncertain by $\approx 30\%$ due to calibration, so their ratios could be off by a factor of two and cannot be used to rule out either mechanism.

Since a straightforward comparison of column densities may be complicated by the differences in beam size of the data in Table 2, we have determined the NH₃ abundance toward NGC 1333 IRAS 4A using the approach of § 3. The same temperature and density structure as in § 3 are used, and the original collisional rate coefficients of Danby et al. (1988). Based on the UMIST database (Le Teuff et al. 2000, www.rate99.co.uk), the rates of the major destruction reactions of NH₃ do not depend on temperature. Formation of NH₃ is mainly by dissociative recombination of NH_4^+ , the rate of which has a $T^{-0.5}$ dependence, which in the model for NGC 1333 IRAS 4A corresponds to a factor of 5. This factor is dwarfed by the exponential increase in H_2D^+ so only constant-abundance models have been considered for NH₃. The observations of Shah & Wootten (2001) are reproduced for $\text{NH}_3/\text{H}_2 = 1 \times 10^{-8}$.

Rodgers & Charnley (2001) present a chemical scheme to form deuterated ammonia in the gas phase, which assumes that the branching ratios of dissociative recombination are statistical and that the relevant reaction rates are isotope-independent. Using this scheme, for $\text{NH}_3/\text{NH}_2\text{D}=10$ (Table 2), an abundance ratio of NH_3/ND_3 of ≈ 10000 is expected. The observed value of $10^{-8}/10^{-11} = 1000$ is inconsistent with this prediction. This disagreement may indicate that a detailed chemical network is needed instead of a statistical treatment. In addition, $\text{NH}_3/\text{NH}_2\text{D}$ was measured in an arcmin-sized region and may be < 10 within the $25''$ CSO beam. Based on the observed NH_3/ND_3 ratio, $\text{NH}_3/\text{NH}_2\text{D}$ could approach unity on small scales.

In the case of surface chemistry, the observed NH_3/ND_3 ratio implies an atomic D/H ratio of ≈ 0.15 in the gas phase (Rodgers & Charnley 2001). This is significantly higher than the values of $10^{-2} - 10^{-3}$ in the chemical models of Roberts & Millar (2000). Based on this discrepancy and on the closer agreement of the observed NH_3/ND_3 ratio with the gas-phase prediction for $\text{NH}_3/\text{NH}_2\text{D}=10$, we tentatively conclude that ion-molecule reactions are presently the preferred formation mechanism of NH₃ in NGC 1333. This mechanism can reproduce the observed deuteration levels if deuterium trans-

fer reactions are much faster than proton transfers. In the future, this conclusion should be tested through measurements of the NH₃, NH₂D, ND₂H and ND₃ abundances in a larger source sample. Any conclusion drawn from such data will be much stronger if the lines are measured with similar beam sizes. More detailed chemical networks are also needed. Such a project could constrain the relative importance of gas-phase and grain-surface deuteration as a function of environment.

Acknowledgements. The CSO is supported by NSF grant AST 99-80846. HSPM acknowledges support from the Deutsche Forschungsgemeinschaft (DFG) via grant SFB 494.

References

- Blake, G. A., Sandell, G., van Dishoeck, E. F., et al. 1995, *ApJ*, 441, 689
- Ceccarelli, C., Castets, A., Loinard, L., Caux, E., & Tielens, A. G. G. M. 1998, *A&A*, 338, L43
- Charnley, S. B., Tielens, A. G. G. M., & Rodgers, S. D. 1997, *ApJ*, 482, L203
- Danby, G., Flower, D. R., Valiron, P., Schilke, P., & Walmsley, C. M. 1988, *MNRAS*, 235, 229
- Dartois, E. & d'Hendecourt, L. 2001, *A&A*, 365, 144
- di Lonardo, G. & Trombetti, A. 1981, *Chem. Phys. Lett.*, 84, 327
- Gibb, E. L., Whittet, D. C. B., Schutte, W. A., et al. 2000, *ApJ*, 536, 347
- Helminger, P. & Gordy, W. 1969, *Physical Review*, 188, 100
- Hogerheijde, M. R. & van der Tak, F. F. S. 2000, *A&A*, 362, 697
- Lacy, J. H., Faraji, H., Sandford, S. A., & Allamandola, L. J. 1998, *ApJ*, 501, L105
- Le Teuff, Y. H., Millar, T. J., & Markwick, A. J. 2000, *A&AS*, 146, 157
- Lis, D. C., Roueff, E., Gerin, M., et al. 2002, *ApJ*, in press
- Loinard, L., Castets, A., Ceccarelli, C., Caux, E., & Tielens, A. G. G. M. 2001, *ApJ*, 552, L163
- Müller, H. S. P., Thorwirth, S., Roth, D. A., & Winnewisser, G. 2001, *A&A*, 370, L49
- Pickett, H. M., Poynter, R. L., Cohen, E. A., et al. 1998, *J. Quant. Spectrosc. Radiat. Transfer*, 60, 883
- Roberts, H. & Millar, T. J. 2000, *A&A*, 361, 388
- Rodgers, S. D. & Charnley, S. B. 2001, *ApJ*, 553, 613
- Roueff, E., Tiné, S., Coudert, L. H., et al. 2000, *A&A*, 354, L63
- Saito, S., Ozeki, H., Ohishi, M., & Yamamoto, S. 2000, *ApJ*, 535, 227
- Shah, R. Y. & Wootten, A. 2001, *ApJ*, 554, 933
- Stark, R., van der Tak, F. F. S., & van Dishoeck, E. F. 1999, *ApJ*, 521, L67
- Turner, B. E. 1990, *ApJ*, 362, L29
- . 2001, *ApJS*, 136, 579
- van der Tak, F. F. S. & van Dishoeck, E. F. 2000, *A&A*, 358, L79

Womack, M., Ziurys, L. M., & Wyckoff, S. 1992, ApJ, 393,
188